SHIRMS 2008 – Y. Potvin, J. Carter, A. Dyskin, R. Jeffrey (eds)
© 2008 Australian Centre for Geomechanics, Perth, ISBN 978-0-9804185-5-2
doi:10.36487/ACG_repo/808_101

Forecasting Seismic Hazard in Mines

A.J. Mendecki *ISS International Limited, South Africa*

Abstract

Probabilistic seismic hazard estimates depend on the parameters of the survival function that describes the size distribution of seismicity: α, β and P_{max}, and on the ground motion relation for a given volume of rock. Parameter α measures the activity rate, β is inversely proportional to the observed mean event size, and the P_{max} is the maximum expected potency. In mines it makes more sense to conceptualise P_{max} as the expected next largest event, which can be estimated from seismic history, or better, seismic history and volume mined V_m. If α is proportional to V_m, and β is constant, as is frequently assumed, then forecasting hazard is straightforward – it is proportional to V_m. There are, however, examples where α increases with V_m in a non-linear way and β decreases with V_m, in which case the future seismic response to mining may accelerate. To forecast seismic hazard we need to extrapolate relations between α, β and V_m into the future, determine the new P_{max} and the expected number of events. A new parameter which measures volume extraction induced seismic strain, ε_{V_m}, is defined to monitor seismic response to mining. It is the ratio of cumulative seismic deformation, $\sum \bar{u}$, to the characteristic length of volume mined, l_{V_m}, over a given period of time, $\varepsilon_{V_m}=0.0012\sum P^{1/3}/l_{V_m}$. It may portend changes in α and β, and its increase with time, or with volume mined, is undesirable. Probabilistic size distribution hazard can easily be extended to ground motion, provided the appropriate prediction equation(s) can be found. Then by calculating probabilities of experiencing damaging ground motion in a certain volume of rock, or the expected cumulative volume of strong ground motion, we may attempt to compare seismic hazard between different mines or areas. The few illustrative examples given do not constitute case studies.

1 Uncertainty, risk, hazard and ground motion

Uncertainty is the existence of more than one possibility and it is measured by a set of probabilities assigned to a set of possibilities. Risk is a state of uncertainty where some of the possibilities involve a loss, and is measured by assigning losses to some possible outcomes. Therefore, one may have uncertainty without risk but not risk without uncertainty. The notion that events are uncertain is both complicated and uncomfortable, therefore we tend to underestimate uncertainty and consequently underestimate risk.

Seismic risk at a given site X can be defined as a product of the probability that a potentially damaging ground motion, v_d, will occur within a given period of time in the future ΔT and the resulting liability $\mathscr{L}(X)$. This probability, $\Pr(\geq \mathrm{v}(X), \Delta T)$, is called seismic hazard or, in this case, strong ground motion hazard. Integrating the product over all possible locations gives the total risk:

$$\mathrm{Risk}(\geq \mathrm{v}_d, \Delta T) = \int_X \{\Pr[\geq \mathrm{v}_d(X), \Delta T] \cdot \mathscr{L}(X)\}\, dX \tag{1}$$

The level of damaging ground motion depends on the type of structure at a given site, therefore it is a function of X. Since probability is dimensionless, seismic risk is expressed in the units of liability $\mathscr{L}$.

In earthquake seismology the probabilistic hazard analysis includes the determination of the volumes that produce seismicity, estimating the recurrence times of seismic events of different magnitude ranges, and taking into account ground motion characteristics, computing the probability of exceeding a given level of ground motion for different time intervals. The results may be presented as a table of probability of each level of ground motion for a given site or as contours of different levels of ground motion at a given level of probability.

Ground motion characteristics include peak ground acceleration (*PGA*), velocity (*PGV*) and displacement (*PGD*). The *PGA* is most convenient for structural engineers, since the maximum force experienced by a rigid structure is F_{max}=*mass*·*PGA*. However, the *PGA* is a poor parameter for evaluating potential for damage. For example, a large *PGA* associated with a high frequency pulse may be absorbed by the inertia of the

structure with little deformation, $PGD \propto PGA/f^2$, where f is frequency. On the other hand, a more moderate acceleration associated with a long duration pulse of low frequency may result in a significant deformation of the structure. The PGV, which is less sensitive to the higher-frequency components of ground motion than PGA, can be measured directly and reliably and provides a reasonable indication of damage potential.

Seismic systems in mines are designed to locate events and to estimate their source parameters: seismic potency P, or seismic moment $M = rigidity \cdot P$, and radiated energy E. Seismic potency for a volume source is the product of the strain change and the source volume, $P=\Delta\varepsilon V$, and for a planar source, the product of an average displacement and source area, $P=\bar{u}A$. One can use $\log P$ as a measure of magnitude: it is simple, reliable, independent of rigidity and thus more portable, therefore one can objectively compare events and seismic hazard between different mines (Mendecki, 2005). For smaller earthquakes in California the relation between the local (Richter) magnitude m_L and potency is simply $m_L=\log P + 0.72$ Ben-Zion and Zhu (2002). Table 1 below compares $\log P$ with Hanks and Kanamori (1979) moment-magnitude, m_M, for rigidity 30 GPa.

Table 1 Logarithm of potency and moment-magnitude

$\log P$	-1	0	1	2	3	4
$m_M = 0.66\log P + 0.92$	0.3	0.9	1.6	2.2	2.9	3.6

The use of energy, E, in seismic hazard estimation would be more appropriate than the use of P or m_L, since it is the radiated energy that drives strong ground motions. However, the estimation of seismic energy from waveforms requires far-field recordings over a wide frequency bandwidth, at least $0.2 \cdot f_0$ to $10 \cdot f_0$, where f_0 is the predominant frequency of a given event at source. Due to the limited aperture of the mine seismic networks, large events are frequently recorded by sensors positioned in the near or intermediate fields of seismic radiation. Also, due to the limited capabilities of the sensors, the frequency bandwidth on both sides of the radiated spectrum is not always available. Moreover, the rate of seismic activity in mines does not always allow for careful, time consuming processing with proper corrections for attenuation and site effects. As a result the estimate of radiated energy is at least twice as uncertain as is seismic potency. Since for small earthquakes magnitude $m \propto \log E \propto \log P \propto \log l$, where l is the source size (Kanamori and Anderson, 1975), the use of potency in size distribution hazard for hard rock mines is acceptable.

To make a reliable estimate of source parameters seismic sensors are placed in boreholes away from the skin of excavations to avoid the very site effects that amplify ground motion at certain frequencies. In such cases we do not measure damaging ground motion and thus seismic hazard analysis is limited to estimating the probabilities of occurrence of seismic events above a certain size.

2 Size distribution hazard and volume mined

2.1 Probability

Over the short term, seismic events tend to occur in bursts or clusters triggered by the internal or external forces producing aftershock sequences. An internal trigger can be provided by a nearby seismic event. External triggers are mining excavations, blasting, fluid injection or even tidal forces. Seismic activity may also build-up and die gradually, generating a swarm of events. Such processes are neither stationary nor independent, nevertheless over longer term such observations may conform to the Poisson process as a result of a number of random superpositions. For example, seismic activity associated with a particular geological structure or with a particular working place may not be stationary at all, but the overall seismicity produced by a number of structures and working places over time may well look stationary. The inter-event time distribution of larger seismic events in most of the mines tested turns out to be random (du Toit and Mendecki, 2007).

For a Poisson process, i.e. a random series of n events occurring in time Δt, and for the activity rate, $n/\Delta t$, which is fixed or is known exactly, the probability that a maximum size event will exceed potency P in time ΔT into the future is:

$$\Pr(\geq P, \Delta T) = 1 - \exp\left[-\Delta T \cdot \frac{n}{\Delta t} \cdot \Pr(\geq P)\right] \quad (2)$$

where $\Pr(\geq P)$ is the complementary cumulative function of the potency-frequency distribution also called the survival function. Since $\Pr(\geq P)$=$N(\geq P)/n$, the Equation (2) gives the recurrence time $\bar{t}(\geq P)$=$\Delta t/N(\geq P)$ or $\bar{t}(\geq P)$=-$\Delta T/\ln[1-\Pr(\geq P,\Delta T)]$, where $\Pr(\geq P,\Delta T)$ is the probability of exceedance, and ΔT is the exposure time. For 5% probability of exceedance and 50 years of exposure the recurrence time is 975 years. The accepted civil engineering criterion is 2% in 50 years, which gives the recurrence time 2475 years.

As we have less data, i.e. as the time of observation and/or the number of events decrease, the statistical uncertainty associated with probability given by Equation (2) must increase. Multiplying the right side of Equation (2) by the posterior density function of the activity rate, and taking the sum of all its possible values, one can account for the uncertainty in the activity rate. Assuming a uniform prior distribution for the activity rate the seismic hazard then is:

$$\Pr(\geq P,\Delta T) = 1 - \left[\frac{\Delta t}{\Delta t + \Delta T \cdot \Pr(\geq P)}\right]^{n+1} \tag{3}$$

The ratio of Equation (3) over Equation (2) is always greater than one and this probability premium drops quickly to one with increase in n (Benjamin, 1968; McGuire, 1977; Campbell, 1982). Replacing ΔT in Equations (2) or (3) with $\bar{t}(\geq P)$, gives the probability $\Pr[\geq P,\bar{t}(\geq P)]$=63%, regardless of potency.

2.2 Survival functions

The most commonly used survival functions of potency-frequency distributions of seismicity are the open-ended (OE) power law, also known as the Gutenberg-Richter relation for magnitudes (Ishimoto and Iida, 1939; Gutenberg and Richter, 1944), the upper-truncated (UT) power law (Page, 1968; Cornell and Vanmarcke, 1969; Cosentino et al., 1977) and gamma-type (GT) distributions (Saito et al., 1973; Vere-Jones, 1976; Main and Burton, 1984; Kagan, 1997; Sornette and Sornette, 1999; Kagan, 2002a; Kagan, 2002b).

OE: The number of events with potency not smaller than P in the OE relation is defined as $N(\geq P) = \alpha P^{-\beta}$, where α and β are parameters. The potency of the one largest event, referred to as the P_{max}, can be derived from $\alpha P_{max}^{-\beta}$=1, that gives P_{max}=$\alpha^{1/\beta}$. The probability of having an event with potency not smaller than P is $\Pr(\geq P)$=$N(\geq P)/N(\geq P_{min})$, which gives:

$$\Pr(\geq P) = P_{min}^{\beta} P^{-\beta} \tag{4}$$

where P_{min} is the threshold potency. The probability density function is $f(P)$=$\beta P_{min}^{\beta} P^{-\beta-1}$. The OE power relation implies scale invariance, i.e. puts no prior limit on the maximum possible event size and for β<1 has infinite values of all statistical moments, including its mean. It exhibits a non-linear growth of cumulative sum of seismic potency with time as $t^{1/\beta}$ (Sornette and Sornette, 1999; Rodkin and Pisarenko, 2006). The total potency production, $P(0,\infty) = N(\geq P_{min}) \int_0^{\infty} P f(P) dP$, where $f(P)$=$d\Pr(\leq P)/dP$ is the probability density function, is infinite. For β<1, which is typical for seismic activity, it can be integrated from zero to a finite potency $P(0,P)$=$\alpha\beta P^{1-\beta}/(1-\beta)$. For β>1 it can be integrated from a finite potency to infinity, $P(P,\infty)$=$-\alpha\beta P^{1-\beta}/(1-\beta)$, and for β=1 it is only finite within the finite potency range, $P(P_1,P_2)$=$\alpha\ln(P_2/P_1)$.

UT: The UT is a version of OE and its survival function is:

$$\Pr(\geq P) = \left(P^{-\beta} - P_{max}^{-\beta}\right) / \left(P_{min}^{-\beta} - P_{max}^{-\beta}\right) \tag{5}$$

with a hard upper limit on potency, P_{max}, such that $\Pr(> P_{max})$=0. The probability density function here is $f(P)$=$\beta P^{-\beta-1} / \left(P_{min}^{-\beta} - P_{max}^{-\beta}\right)$. The equations for potency production are the same as in case of the OE distribution, with the exception that we can integrate only up to P_{max}.

GT: The GT relation is a product of the OE survival function and an exponential taper which constitute a soft limit P_{max} above which the probability decays quickly but is finite, therefore $\Pr(> P_{max})$>0. The survival function of the GT is:

$$\Pr(\geq P) = \frac{C(P)}{C(P_{min})} P_{min}^{\beta} P^{-\beta} \exp\left(\frac{P_{min} - P}{P_{max}}\right) \tag{6}$$

where: $C(P)/C(P_{min})$ is the normalising factor, $C(P) = 1-(P/P_{max})^{\beta}\exp(P/P_{max})\Gamma(1-\beta, P/P_{max})$ and $\Gamma(1-\beta, P/P_{max}) = \int_{P/P_{max}}^{\infty} t^{-\beta}\exp(-t)\,dt$. For $\beta < 1$ the total potency production over the potency domain from zero to infinity is finite, $P(0,\infty)$=$\alpha\beta P_{max}^{1-\beta}\Gamma(1-\beta)$.

All three survival functions are part of so-called thick-tail distributions, where probabilities of extreme events are relatively high. Figure 1 compares the three survival functions with the exponential, which is a thin-tail distribution. The probability to exceed $\log P$=2.0 for the OE distribution is 1.0%, for the UT it is 0.9%, for GT is 0.82% and for exponential 10^{-50}%. Figure 1 also shows the influence of the assumed $\log P_{max}$ on recurrence times in the data set: Δt=847 days, n=1637 and $\log P_{maxo}$=2.7. A change in the assumed $\log P_{max}$ by 0.5 units may influence the estimated recurrence times of larger events by few hundred per cent.

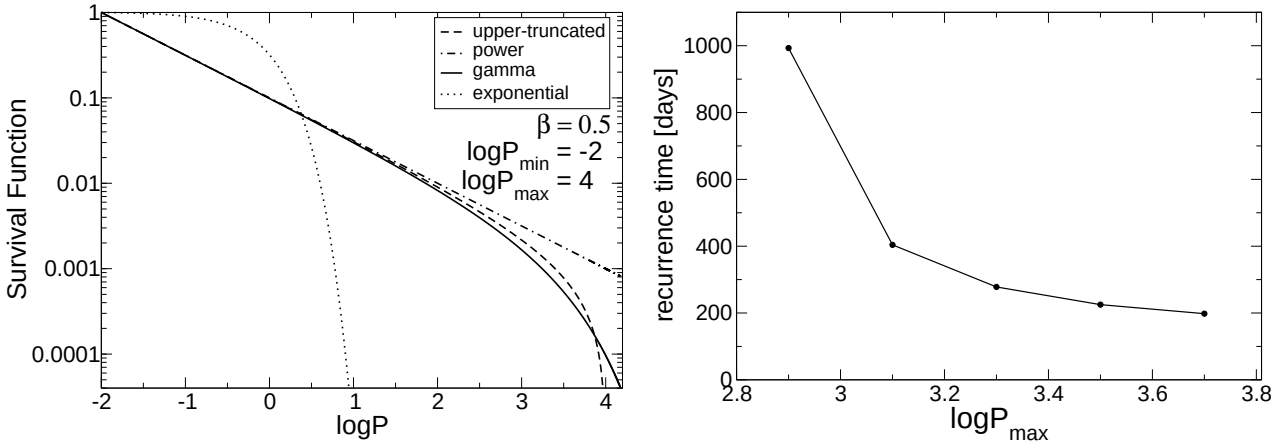

Figure 1 Comparison of thick-tail survival functions: OE, UT and GT versus the thin-tailed exponential, for the same set of parameters (left). An example of the influence of P_{max} on the recurrence times of larger events (right)

2.3 The maximum event size: P_{max}

P_{max} is the maximum event potency above which the probabilities of occurrence are zero or negligibly small. It may be defined as the size of the largest event ever possible, or the next P_{max}, or as the maximum event to close the deficit of deformation due to the effective volume mined $P_{max}(V_{meff})$. P_{max} is poorly constrained by data but it has a significant influence on the estimated hazard.

2.3.1 P_{max} and past seismic activity

Let's ask the following question: given a set of observations in chronological sequence, how often will the outstanding value (the record value) be surpassed? The expected number of record highs in a chronological sequence of n independent observations is the sum $\sum_{j=1}^{n}(1/j)$. The same applies if we run the sequence in reverse, i.e. from most recent back to the oldest observation. This harmonic sequence grows without bound, though rather slowly (Oresme, 1482). This supports the idea that any record can be beaten, but the time for this becomes longer and longer with the increasing number of records. It may surprise that 1000 random observations gives only 7.49 record highs (or lows) and 1000000 observations gives only 14.39. Chandler (1952) showed that the probability of 10 or more record highs in a 100 long random sequence is less than 5%. Foster and Stuart (1954) suggested that the observed frequencies of record highs (or lows) can be used to infer whether or not the data set is random. It is interesting to note that by this criterion the data used in this paper as examples turned out to be random: SA1 has 5383 observations and 11 records (versus 11.66 theoretical), SA2 has 1921 observations and 7 records (8.13), AU1 has 5193 observations and 9 records (9.13) and EU1 has 1174 observations and 8 records (7.64). However, taking the three months, November 2006 to February 2007, at SA1 we have 402 observations and 11 records versus 6.57 theoretical, which is anything but random. The reason may be the small sample of data or the degraded system stiffness implied by lower β-value at that time.

For systems driven steadily over long periods of time the sequence of records will be a monotonously increasing function of time with decreasing gradient, which is the case in crustal seismology. The problem then may be reduced to finding the truncation point, $\log P_{max}$, of the distribution from n data points. An obvious estimator is $\log P_{maxo}$ – the largest observed seismic event in the complete data set, that will always underestimate $\log P_{max}$, but the bias should decrease as the size of the data set increases. Robson and Whitlock (1964) show that the bias correcting term is the difference between the size of the largest and the second largest value:

$$\log P_{max} = \log P_{maxo} + (\log P_{maxo} - \log P_{maxo-1}) \tag{7}$$

where $\log P_{maxo-1}$ is the second largest observed potency. The disadvantage of this estimator is that only the two largest observed seismic events are used. It makes intuitive sense to use the weighted average of the differences in an ordered data set as the biased correcting term. This is the best estimator in the mean square error sense if no assumption is made about the type of distribution (Cooke, 1979):

$$\log P_{max} = \log P_{maxo} + \left[\log P_{maxo} - \left(1 - e^{-1}\right) \sum_{j=0}^{n-1} e^{-j} \log P_{maxo-j}\right] \tag{8}$$

If the size distribution follows the well-known power-law, then the best estimator is:

$$\log P_{max} = \log P_{maxo} + \int_{\log P_{min}}^{\log P_{max}} \left(\frac{10^{-\beta \log P_{min}} - 10^{-\beta \log P}}{10^{-\beta \log P_{min}} - 10^{-\beta \log P_{max}}}\right)^n d(\log P) \tag{9}$$

which can be solved iteratively (Kijko, 2004).

In mines, however, the driving forces are not steady and the sequence of the record highs may be jerky. Then the difference between $\log P_{maxo}$ and the future $\log P_{max}$ may not necessarily decrease with the size of the data set, or with the volume mined. In such a case the $\log P_{max}$ may be interpreted as the potency of the next largest event, as opposed to the largest ever possible, and the conservative bias correcting term can be taken as:

$$\log P_{max} = \log P_{maxo} + \max(\Delta \log P_{maxo}) \tag{10}$$

where $\max(\Delta \log P_{maxo})$ is the maximum observed jump in the log of the observed series of record potencies. Since mining scenarios may change, it is advisable to select the past data that is most relevant to future mining.

Table 2 summarises results of P_{max} estimation for the four data sets. Based on a number of cases the two recommended methods are given by Equation (9), or more conservatively Equation (10).

Table 2 The maximum potency estimation from past data

	Estimated $\log P_{max}$ and the Range						
Data Set	$\log P_{maxo}$	Eq(7)	Eq(8)	Eq(9)	Eq(10)	OE	Range
SA1	3.5	4.3	3.8	3.7	4.3	4.4	0.7
SA2	2.6	2.6	2.6	2.7	3.3	4.5	0.9
AU1	2.2	3.1	2.6	2.7	3.2	2.5	0.7
EU1	2.5	3.0	2.7	2.7	3.1	2.9	0.4

2.3.2 P_{max} and volume mined

If we assume that the extraction of rock, the back-fill placement, and the seismic and aseismic deformation take place within the volume ΔV at discrete times, then we can construct the following step function that reflects a balance of inelastic deformation:

$$B(t) = V_m(t) - V_b(t) - V_P(t) - V_a(t) \tag{11}$$

where: $V_m(t) = \sum_{t_i \le t} V_m(t_i)\,\Theta(t - t_i)$ is the cumulative volume mined to date, $V_m(t_i)$ is the volume mined at t_i, $V_b(t) = \sum_{t_j \le t} c_b(t)\, V_b(t_j)\,\Theta(t - t_j)$ is the cumulative volume of backfill placed to date, where $V_b(t_j)$ is backfill

placed at t_j, $V_{meff}(t) = V_m(t) - V_b(t)$ is called the effective volume mined to date, $c_b(t)$ is the efficiency of back-fill that corrects for shrinkage and compaction, $V_P(t) = \gamma_0 \sum_{t_k \le t} P(t_k)\,\Theta(t-t_k)$ is the cumulative volume reduction associated with seismic inelastic deformation to date, $P(t_k)$ is the seismic potency of the event at time t_k, $P_I(t_k)$ is the isotropic component of the potency $P(t_k)$, $\gamma_0 = P_I(t_k)/P(t_k)$, is the portion of the isotropic component of the total scalar potency associated with seismic activity close to excavations, which for events close to excavation faces $0.6 \le \gamma_0 \le 0.9$ (McGarr, 1993), $V_a(t) = \gamma_a \sum_{t_l \le t} P(t_k)\,\Theta(t-t_k)$ is the cumulative volume of aseismic inelastic deformation to date, spatially and temporarily synchronous with seismic activity, where $\gamma_a = P_a(t_k)/P(t_k)$, and $P_a(t_k)$ is the aseismic potency at t_k, Θ is the Heaviside function, $\Theta(t)$=0 if t<0, and $\Theta(t)$=1 if $t \ge 0$. The Equation (11) can now be written as:

$$B(t) = V_{meff}(t) - (\gamma_0 + \gamma_a) \sum_{t_k \le t} P(t_k)\,\Theta(t-t_k) \tag{12}$$

and we can consider two scenarios for the P_{max}.

Scenario 1 - collapse. The current deficit of deformation $B(t)$ is to be closed in a single large seismic event, which may or may not fit to the observed power law size distribution. This can be consider the worst case scenario, however, history shows that it is possible to engineer such a pathological mining layout that at some stage collapses in one large seismic event. Without external loading the maximum potency of such an event would be limited to:

$$P_{max}(V_{meff}, t) = B(t) = V_{meff}(t) - (\gamma_0 + \gamma_a) \sum_{t_k \le t} P(t_k)\,\Theta(t-t_k) \tag{13}$$

Scenario 2 - power law deficit closure. The deficit of deformation is closed due to seismic activity with power law size distribution. In this case P_{max} can be estimated from the Equation (13) by replacing the sum of seismic potency by a model of potency production derived from the size distribution:

$$\sum_{t_k \le t+\Delta T} P(t_k)\,\Theta(t-t_k) = C(\alpha,\beta)\,P_{max}^{1-\beta} \tag{14}$$

where $C(\alpha,\beta) = \alpha\beta/(1-\beta)$ for the OE and UT distributions and $C(\alpha,\beta) = \alpha\beta\Gamma(1-\beta)$ for the GT distribution.

The balance is now a function of the effective volume mined and the parameters of the model:

$$B(t;\alpha,\beta) = V_{meff}(t) - (\gamma_0 + \gamma_a)\,C(\alpha,\beta)\,P_{max}^{1-\beta} \tag{15}$$

where α and β are derived from the maximum likelihood fit to data. By setting $B(t;\alpha,\beta) = 0$ we can now calculate the P_{max} of the potency-frequency distribution that would have closed the deficit of deformation:

$$P_{max}(V_{meff}, t) = \left[\frac{1}{C(\alpha,\beta)} \cdot \frac{V_{meff}(t)}{(\gamma_0 + \gamma_a)} \right]^{\frac{1}{1-\beta}} \tag{16}$$

Similar equations were derived by Wyss (1973), Smith (1976), McGarr (1976) and Molnar (1979) to estimate the expected maximum magnitude of earthquakes, and by McGarr (1984) for mines. The interpretation of Equation (16) seems straightforward: $P_{max}(V_{meff}, t)$ increases with the effective volume mined. For given $V_{meff}(t)$ the more seismic and aseismic potency has been produced to date, i.e. higher α, lower β and higher γ_a, the less there is to be produced to close the deficit, therefore, the P_{max} gets lower. For a well behaved data set and no external loading on the system the Equation (16) should deliver $P_{max} \le B(t)$.

Figure 2 shows an example of the balance graph and its statistics at SA1. The graph shows the cumulative effective volume mined, the balance of deformation, the cumulative potency production, the volume mined seismic strain and its long-term average. From October 2004 to February 2007 the OE estimate of $\log P_{max}$ increased from 3.7 to 3.9, while, as a result of a few larger events and a slower rate of mining during that time,

$\log P_{max}\,(V_{meff})$ decreased, as expected, from 3.8 ($\log B = 3.9$) to 3.7 ($\log B = 3.7$). There is no reason, except for external loading, why after having a few large events and with significantly lower production the P_{max} should increase. The volume mined for the other data sets was not available.

A new parameter which measures volume extraction induced seismic strain, ε_{V_m}, is defined to monitor seismic response to mining. It is the ratio of cumulative seismic deformation, $\sum \bar{u}$, to the characteristic length of volume mined, l_{V_m}, over a given period of time. The size of a circular source can be approximated from the Eshelby (1957) solution, $l=(3.5P/\Delta\varepsilon)^{1/3}$, where $\Delta\varepsilon$ is an average strain change at the source. Inserting it into $P=\bar{u}\pi\,(l/2)^2$ gives $\bar{u}=0.5524\Delta\varepsilon^{2/3}P^{1/3}$, and for $\Delta\varepsilon=10^{-4}$ we have $\bar{u}=0.0012P^{1/3}$. Taking the characteristic length of a given volume mined as $l_{V_m}=V_m^{1/3}$ gives:

$$\varepsilon_{V_m} = \sum \bar{u}/l_{V_m} = 0.0012 \sum P_j^{1/3}/V_m^{1/3} \tag{17}$$

In this example the ε_{V_m} increased slowly with steady production since the beginning of 2006. Notwithstanding a lower production rate since late October 2006, the ε_{V_m} continued increasing over its long-term average until the discharge of a few large potency events at the end of January 2007. Note that the record $\log P$=3.5 occurred almost immediately after the previous record of 2.7 and relatively quickly after the 2.5 record event.

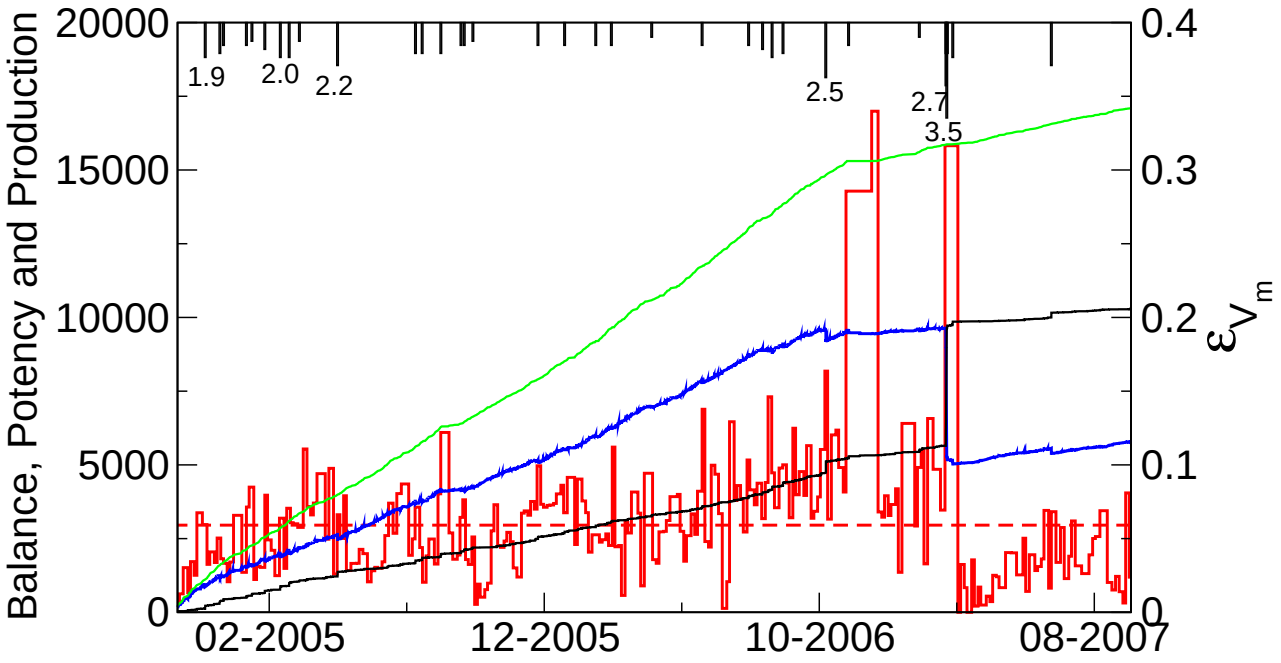

Figure 2 **Balance graph for SA1 that includes the cumulative effective volume mined V_{meff} (top line), the balance of deformation B with c_b=0.5, γ_a=0.2, γ_0=0.9 (second from the top), the cumulative potency production $\sum P$ (third from the top) and the ε_{V_m} with its long-term average (bottom jerky line). The timing of events with $\log P \geq$1.5 and record $\log P_{max}$'s, versus time (1.9, 2.0, 2.2, 2.5, 2.7, 3.5) are shown on top**

2.4 Future hazard

Parameters α, β and P_{max} of the survival function are derived from past data. But the driving forces of seismic activity, and therefore the parameters of the survival function, are not always constant in time, as may be assumed in crustal seismology.

Mining induced stresses in the rock mass are anything but constant, they are influenced more by commodity prices than by tectonic forces. Under stable rock mass conditions, when the overall stiffness of the rock mass is being maintained, the seismic response to mining, measured by cumulative potency or by the rate of seismic activity, is expected to be proportional to the volume mined. As mining progresses and the overall stiffness of

the rock mass is being degraded the rate of potency release may increase. With further degradation in stiffness the response may become non-linear with accelerating potency production and/or accelerating activity rate. The parameters of the survival function, α, β and P_{max}, are therefore expected to be a function of the effective volume mined to date V_{meff} (Mendecki, 2001).

The data analysed to date shows that the β-value of the potency-frequency distribution is either constant or a decreasing function of the volume mined V_m. In most cases α has shown to be, as expected, proportional to V_m, though at different rates in different areas. However, there are examples where α increases with V_{meff} in a non-linear way. Figure 3 shows the behaviour of α and β versus V_m in South African mines and versus time, as a proxy, in two Australian mines.

By extrapolating the observed relationship between α, β and the volume mined, or time, see dotted lines at Figure 3, we can forecast future hazard for different production scenarios from Equation (3):

$$\Pr\left[\geq P, V_m\left(\Delta T\right)\right] = 1 - \left[\frac{1}{1+\Pr\left[\geq P, \alpha\left(\Delta T\right), \beta\left(\Delta T\right)\right]}\right]^{n[\alpha(\Delta T),\beta(\Delta T)]+1} \tag{18}$$

where $\Pr\left[\geq P, \alpha\left(\Delta T\right), \beta\left(\Delta T\right)\right]$ is the estimated survival function and $n\left[\alpha\left(\Delta T\right), \beta\left(\Delta T\right)\right]$ is the estimated number of events, given the extrapolated values of α and β.

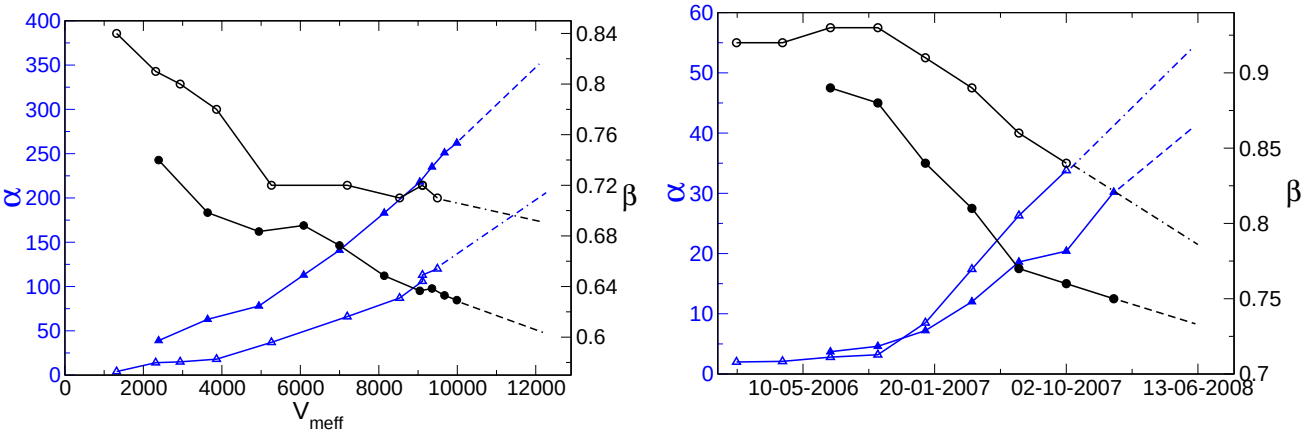

Figure 3 Parameters α (triangles) and β (circles) versus the effective volume mined for two South African mines (left) and versus time for two Australian mines (right)

3 Ground motion hazard

The maximum ground motions experienced at a site are controlled by the maximum velocity of deformation at source (slip velocity), the interaction of radiation from different parts of the source and from different travel paths, and by the site effects.

The near source velocity of ground in a wave radiated is equal to half the slip velocity. Slip velocity can be expressed as a ratio of the effective stress (an initial stress minus resistance to deformation), to seismic impedance, $\dot{u}=\sigma_{eff}/(\rho v_S)$. In such a case the upper limit of ground motion imposed by slip velocity is defined by the bulk shear strength of the rock mass, $\sigma_{bss} \leq \sigma_{eff}$, and for σ_{bss}=60 MPa and ρ=2700 kg/m^3 the $PGV_{max} \leq$3.2 m/s. There is practically no limit on peak ground acceleration though, since fracture in a continuum may produce a steep change in velocity which results in high acceleration at high frequencies (Bommer et al., 2004; Andrews et al., 2007).

The near-source ground motion may be significantly affected by rupture directivity effects and by the permanent displacement called fling step (Archuleta and Hartzell, 1981; Somerville et al., 1997). Since these effects are observed only at specific sites they are not recorded frequently and may not be captured by the ground motion prediction relation.

As an outgoing stress pulse travels away from the source its amplitude is decreasing due to geometrical spreading, inelasticity, and scattering. In perfectly elastic media there is no attenuation and the wave energy is conserved as it propagates. In a spherical body wave of radius R the energy is spread out over its surface and the energy density is $E/\left(4\pi R^2\right)$. Since the energy density is proportional to the square of the measured amplitude of ground velocity $E/\left(4\pi R^2\right)\propto \mathrm{v}^2$, it translate to $\mathrm{v}\propto 1/R$ decay for amplitude with distance. In a surface wave the energy is spread along the perimeter of a circle, the energy density is $E/(2\pi R)$, which leads to $1/\sqrt{R}$ decay for amplitude. The difference between $1/R$ amplitude decay for body waves and $1/\sqrt{R}$ for surface waves is significant, specifically at larger distances. A simple, functional prediction equation for the *PGV* caused by an event of potency P at distance R is $PGV=cP^{c_P}\left(R+c_l P^{1/3}\right)^{-c_R}$, or in a logarithmic form:

$$\log PGV = c_P \log P - c_R \log\left(R + c_l P^{1/3}\right) + \log c \tag{19}$$

where c_P is the potency dependence parameter, c_R is the geometrical spreading and attenuation parameter and c is a free constant (Kanai, 1961; Campbell, 1981). The term $c_l P^{1/3}$ is introduced to saturate the near-source ground motion and is expressed as a fraction of the source size, say (0.1 to 0.5)l, at which peak ground velocity remains steady. The size of the circular source can be estimated from the classical Eshelby (1957) solution, $l=(3.5P/\Delta\varepsilon)^{1/3}$, and for the strain change at the source $\Delta\varepsilon=10^{-4}$ this gives c_l=3.3 to 16.3. For c_R=1.0, i.e. geometrical spreading $1/R$ with no attenuation and for c_l = 0, the Equation (19) gives the familiar $\log(R\cdot PGV)=c_P \log P+\log c$.

To get a sensible prediction equation we need to prepare a sensible data set, which is not easy because the *PGV* are not always well distributed with respect to potencies (or energies) and distance. The inversion procedure for parameters in Equation (19) should be carried out in two stages to decouple potentially correlated variables, in this case c_P and c_R, otherwise errors in potency determination may affect the distance coefficient (Joyner and Boore, 1993; 1994). Adding the mean square error to the constant c provides a more conservative prediction of the peak ground velocity, see grey lines on Figure 5.

Probability of PGV. To calculate the probability that the $PGV\geq \mathrm{v}$ at the distance R from a source we need to replace the potency P in the survival function with P derived from Equation (19), for example $P=(\mathrm{v}/c)^{1/c_P} R^{c_R/c_P}$ for c_l=0. Assuming the UT distribution it gives:

$$\Pr(\geq \mathrm{v}, R) = \frac{1}{P_{min}^{-\beta} - P_{max}^{-\beta}} \left[\left(\frac{c}{\mathrm{v}}\right)^{\beta/c_P} R^{-\beta c_R/c_P} - P_{max}^{-\beta} \right] \tag{20}$$

If we further assume that the spatial distribution of seismicity within the volume of interest is uniform, then the probability that a given site will experience $PGV\geq \mathrm{v}$ due to event within the distance between R_1 and R_2 can be estimated from the following formula:

$$\Pr(\geq \mathrm{v}; R_2 - R_1) = \frac{1}{R_2 - R_1} \int_{R_1}^{R_2} \Pr(\geq P, R)\, dR \tag{21}$$

where $\Pr(\geq P, R)$ is given by the survival function of the potency-frequency distribution with P derived from the ground motion Equation (19). For the UT distribution and c_l=0 there is an analytical solution:

$$\Pr(\geq \mathrm{v}; R_2 - R_1) = \frac{1}{P_{min}^{-\beta} - P_{max}^{-\beta}} \left[\left(\frac{c}{\mathrm{v}}\right)^{\beta/c_P} \frac{R_2^{1-\beta c_R/c_P} - R_1^{1-\beta c_R/c_P}}{(1-\beta c_R/c_P)(R_2 - R_1)} - P_{max}^{-\beta} \right] \tag{22}$$

which, for P_{max}=∞ converges to the OE solution. For $c_l\neq 0$ the potency P can not be derived from Equation (19) directly and this case, as well as the GT distribution, needs to be treated numerically. Equation (22) can now be inserted into Equation (3) to estimate the probability that the volume of rock delineated by radii R_1 and R_2 from a given site will experience $PGV\geq \mathrm{v}$ within the future time ΔT. For consistency, the ground motion parameters, c_P, c_R and c, and size distribution parameters, α, β and P_{max} should be derived from a data set covering the same area and the same period of time. Figure 4 shows examples of size distribution hazard.

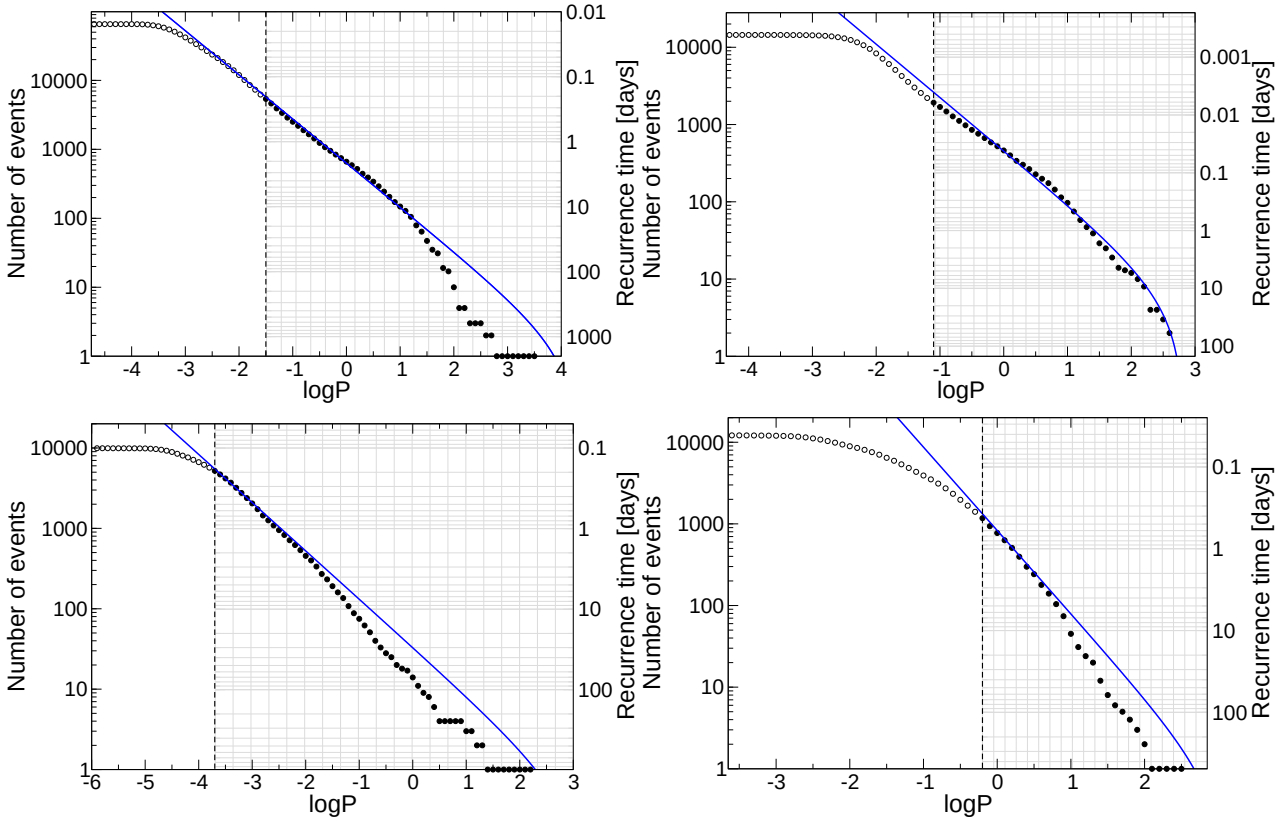

Data Set	α/90 days	β	$\log P_{maxo}$	$\log P_{max}$, Eq(10)	$P(10,P_{max}$; 90 days), m^3	Pr($\geq$2.5, 90 days)
SA1	48	0.64	3.5	4.3	2817	0.64
SA2	345	0.59	2.6	3.3	9916	0.99
AU1	3	0.60	2.2	3.2	74.4	0.06
EU1	151	1.0	2.5	3.1	730.2	0.25

Figure 4 The UT potency-frequency distribution for SA1 and SA2 (top left and right), an AU1 (bottom left) and EU1 (bottom right). Results of size distribution hazard are summarised in the table below the figure

Volume of PGV. From Equation (19) we can estimate the volume of rock subjected to $PGV \geq$v due to an event with potency P:

$$V_{gm}(PGV \geq \mathrm{v}, P) = \frac{4\pi}{3}\left[\left(\frac{c}{\mathrm{v}}\right)^{1/c_R} P^{c_P/c_R} - c_l P^{1/3}\right]^3 \tag{23}$$

To compare seismic hazard in mines with different size distributions and ground motion attenuation one can integrate both, the ground motion prediction equation and the size distribution, into one parameter (Mendecki, 1985; Kijko and Funk, 1994; Eneva et al., 1996). The cumulative volume of ground motion due to all events in the potency range from P_1 to P_2 can be given by $V_{cgm}(\geq \mathrm{v}) = N(\geq P_{min}) \int_{P_2}^{P_1} V_{gm}(\geq \mathrm{v}, P) f(P) dP$, which for OE or UT size distributions is:

$$V_{cgm}(PGV \geq \mathrm{v}) = \frac{4}{3}\pi\alpha\beta \left\{ \frac{\left(\frac{c}{\mathrm{v}}\right)^{3/c_R}}{\frac{3c_P}{c_R} - \beta} \cdot I_1 - \frac{3c_l \left(\frac{c}{\mathrm{v}}\right)^{2/c_R}}{\frac{2c_P}{c_R} + \frac{1}{3} - \beta} \cdot I_2 + \frac{3c_l^2 \left(\frac{c}{\mathrm{v}}\right)^{1/c_R}}{\frac{c_P}{c_R} + \frac{2}{3} - \beta} \cdot I_3 + \frac{c_l^3}{1-\beta} \cdot I_4 \right\} \tag{24}$$

where:
$I_1 = \left(P_2^{-\beta+3c_P/c_R} - P_1^{-\beta+3c_P/c_R}\right)$, $I_2 = \left(P_2^{-\beta+1/3+2c_P/c_R} - P_1^{-\beta+1/3+2c_P/c_R}\right)$, $I_3 = \left(P_2^{-\beta+2/3+c_P/c_R} - P_1^{-\beta+2/3+c_P/c_R}\right)$, $I_4 = \left(P_2^{1-\beta} - P_1^{1-\beta}\right)$. P_1 may be the minimum potency that may cause damage and P_2 the maximum observed or the next maximum expected event size, P_{max}.

For $c_R = 1$ and $c_l = 0$ Equation (24) gives:

$$V_{cgm}(PGV \geq \mathrm{v}) = \frac{4\pi\alpha\beta c^3}{3\mathrm{v}^3(3c_P - \beta)}\left(P_2^{3c_P-\beta} - P_1^{3c_P-\beta}\right) \tag{25}$$

The $V_{cgm}(PGV \geq \mathrm{v})$ for the GT distribution needs to be integrated numerically. Figure 5 shows examples of ground motion hazard.

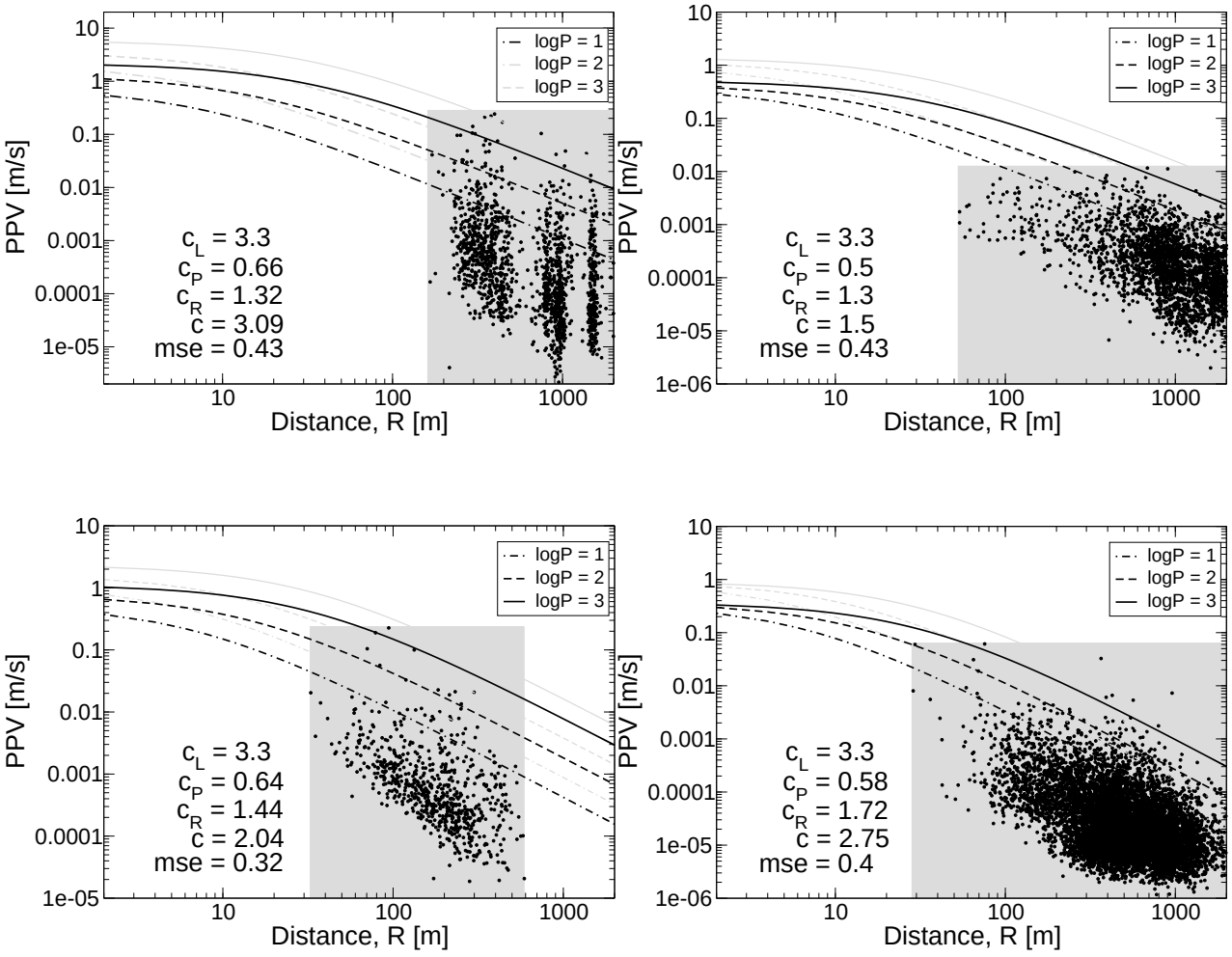

Data Set	$PGV(\log P{=}3;$ 100 m), m/s	Pr($PGV \geq 0.15$; 500-10m, 90 days)	$V_{cgm}(PGV \geq 0.15$, 90 days), m^3
	Eq(19)	Eq(22) and (3)	Eq(24)
SA1	0.46	0.795	$35.5{\cdot}10^6$
SA2	0.09	0.804	$5.8{\cdot}10^6$
AU1	0.15	0.014	$0.16{\cdot}10^6$
EU1	0.03	0.128	$0.23{\cdot}10^6$

Figure 5 ***PGV*** **predictions for SA1 and SA2 data sets (top left and right), and AU1 and in EU1 (bottom left and right), shown here only for** $\log P$**=1, 2 and 3 by black lines. In all cases data was recorded by three component geophones installed in boreholes drilled from underground excavations. The regression plus the mean square error are shown by grey lines. The grey areas indicate the domain of data and dots inside the data used in regression for all event sizes. Results of ground motion hazard are summarised in the table below the figure**

4 Final remarks

If liabilities are attached to probabilities we can calculate seismic related risk, which is not without its problems, and then focus on risk management. Frequently, however, potential liabilities or even historical losses associated with larger seismic events are either unknown or very uncertain. Then the process is even more difficult, we need to interpret seismic hazard in terms of probability, which involves judgment under uncertainty.

In judging uncertain events people rely on a limited number of heuristic principles: rules of thumb, educated guesses, intuitive judgments, experience-based reasoning or simply on common sense. These rules reduce the complex tasks of assessing probabilities values to simpler judgmental operations, which are quite useful, but sometimes they lead to severe and systematic errors (Tversky and Kahneman, 1974; Kahneman, 2003). Our understanding of how judgment works is far from satisfactory. The famous quotation attributed to Mark Twain *"good judgment comes from experience but experience comes from bad judgment"* is hardly comforting. Neither is the one by Pierre-Simon Laplace (1812) *"probability theory is nothing but common sense reduced to calculations",* that relates more to the process of calculating probabilities rather than to their interpretation.

Our common sense, for example, does not extend too far into the very small and into the extreme degrees of likelihood, e.g. $\Pr(\geq 2.5, 120\,\text{days}) = 0.06$ may be difficult to judge. We do not discern well between, say, 0.01 and 0.06 probabilities of having a large event, and tend to underweight larger and overweight smaller probabilities, making little difference in preventative measures between these two cases (Tversky and Kahneman, 1986).

Our common sense also misinterprets clustering. For example, in a Poisson process the time intervals between events of a given size are exponentially distributed. This means that short intervals are more probable than long ones and events tend to cluster in small groups, separated by longer spacings. This apparent clustering does not indicate any greater dependence between the closer-spaced events than between the more distant ones. The common intuitive assumption that randomness in time should lead to uniform spacing of events is erroneous (Lomnitz, 1974).

There is also an uncertainty in probability determination, and to take it into account in the decision making process we need a second number. One option is to partition the probability values into the most likely and the most unlikely domains and quote the range, e.g. $\Pr(\geq 2.5, 120\,\text{days}) = 0.01$ - 0.15.

Human judgment under uncertainty also involves motivational bias, which may be even more critical than statistical misconceptions or errors. In some cases an expert may be motivated by incentives to see things in a certain way. But most frequently an expert is defensively conservative, or may want to suppress uncertainty in order to appear authoritative or knowledgeable, or has taken a strong stand in the past and wants to be consistent. In addition there may be a conflict of interest between the loyalty demanded by the organisation the expert represents or even by the client he consults for, and the expert's objectivity. For more on motivational bias and on duality between probability as frequency and probability as belief see Hogarth (1975) and Vick (2002).

To alleviate some of these problems it is advisable to monitor selected hazard parameters systematically and react to temporal changes rather than to interpret the magnitude of probability at any given time. It is also useful to peer review the methodology, procedures and results.

The probabilistic seismic hazard analysis takes into account all potentially damaging events with a finite probability of occurrence. It is therefore more applicable for seismic risk analysis associated with intermediate size events where damage, though more frequent, is mostly observed close to their sources. The rupture directivity and strong asymmetrical ground motion pattern associated with large events may considerably influence the spatial distribution of damage even at more distant sites. To assess damage potential to the critical structures it is advisable to perform deterministic hazard analysis, that includes simulation of ground motion caused by a few of the largest possible events that may occur at specific locations. The likely locations of these events may be inferred from past seismic activity, can be determined by numerical modelling or may be assumed as the worst plausible scenario for a particular structure.

Acknowledgement

The Size Distribution Hazard and Volume Mined part of the paper is a result of the research project sponsored by the Mine Health and Safety Council of South Africa. I wish to acknowledge useful and insightful discussions with my colleague Cornel du Toit, he also helped with illustrative examples.

References

Andrews, D.J., Hanks, T.C. and Whitney, J.W. (2007) Physical limits on ground motion at Yucca Mountain. Bulletin of the Seismological Society of America, 97(6), pp. 1771–1792.

Archuleta, R.J. and Hartzell, S.H. (1981) Effects of fault finiteness on near-source ground motion. Bulletin of the Seismological Society of America, 71(4), pp. 939–957.

Ben-Zion, Y. and Zhu, L. (2002) Potency-magnitude scaling relation for southern California earthquakes with 1.0<M<7.0. Geophysical Journal International, 148, pp. F1–F5.

Benjamin, J.R. (1968) Probabilistic model for seismic force design. Journal of Structural Engineering ASCE, 94 (ST5), pp. 1175–1196.

Bommer, J.J., Abrahamson, N.A., Strasser, F.O., Pecker, A., Bard, P.Y., Bungum, H., Cotton, F., Fah, D., Sabetta, F., Scherbaum, F. and Studer, J. (2004) The challenge of defining upper bounds on earthquake ground motions. Seismological Research Letters, 75(1), pp. 82–95.

Campbell, K.W. (1981) Near-source attenuation of peak horizontal acceleration. Bulletin of the Seismological Society of America, 71(6), pp. 2039–2070.

Campbell, K.W. (1982) Bayesian analysis of extreme earthquake occurrences. Part 1: Probabilistic hazard model. Bulletin of the Seismological Society of America, 72(5), pp. 1689–1705.

Chandler, K.N. (1952) The distribution and frequency of record values. Journal of the Royal Statistical Society, Series B (Methodological), 14(2), pp. 220–228.

Cooke, P. (1979) Statistical inference for bounds of random variables. Biometrica, 66(2), pp. 367–374.

Cornell, C.A. and Vanmarcke, E.H. (1969) The major influences on seismic risk. In Proceedings 4th World Conference on Earthquake Engineering, Santiago, Chile, pp. 69–83.

Cosentino, P., Ficarra, V. and Luzio, D. (1977) Truncated exponential frequency-magnitude relationship in earthquake statistics. Bulletin of the Seismological Society of America, 67(6), pp. 1615–1623.

du Toit, C. and Mendecki, A.J. (2007) Examples of time distribution of seismic events in mines (Extended Abstract). In 24 IUGG General Assembly, Induced Seismicity Workshop, Perugia, Italy.

Eneva, M., van Aswegen, G. and Mendecki, A.J. (1996) Volume of ground motion and seismic hazard. International Journal of Rock Mechanics and Mining Sciences and Geomechanics Abstract, 35(4), pp. 393–394.

Eshelby, J.D. (1957) The determination of the elastic field of an ellipsoidal inclusion and related problems. Proceedings of the Royal Society of London, Series A, Mathematical and Physical Sciences, 241(1226), pp. 376–396.

Foster, F.G. and Stuart, A. (1954) Distribution-free tests in time-series based on the breaking of records, with discussion. Journal of the Royal Statistical Society, 16(B), pp. 1–22.

Gutenberg, B. and Richter, C.F. (1944) Frequency of earthquakes in California. Bulletin of the Seismological Society of America, 34, pp. 185–188.

Hanks, T.C. and Kanamori, H. (1979) A moment magnitude scale. Journal of Geophysical Research, 84, pp. 2348–2350.

Hogarth, R. (1975) Cognitive processes and the assessment of subjective probability distribution. Journal of the American Statistical Association, 70(350), pp. 271–289.

Ishimoto, M. and Iida, K. (1939) Observations of earthquakes registered with the microseismograph constructed recently (in Japanese). Bulletin of the Earthquake Research Institute of Tokyo University, 17, pp. 443–478.

Joyner, W.B. and Boore, D.M. (1993) Methods for regression analysis of strong motion data. Bulletin of the Seismological Society of America, 83(2), pp. 469–487.

Joyner, W.B. and Boore, D.M. (1994) Methods for regression analysis of strong motion data - Errata. Bulletin of the Seismological Society of America, 84(3), pp. 955–956.

Kagan, Y.Y. (1997) Seismic moment-frequency relation for shallow earthquakes: Regional comparison. Journal of Geophysical Research, 102(B2), pp. 2835–2852.

Kagan, Y.Y. (2002a) Seismic moment distribution revisited: I. Statistical results. Geophysical Journal International, 148(3), pp. 520–541.

Kagan, Y.Y. (2002b) Seismic moment distribution revisited: II. Moment conservation principle. Geophysical Journal International, 149(3), pp. 731–754.

Kahneman, D. (2003) A perspective on judgment and choice - Mapping bounded rationality (Nobel Lecture). American Psychologist, 58(9), pp. 697–720.

Kanai, K. (1961) An empirical formula for the spectrum of strong earthquake motions. Bulletin of the Earthquake Research Institute of Tokyo University, 39, pp. 85–95.

Kanamori, H. and Anderson, D.L. (1975) Theoretical basis of some empirical relations in seismology. Bulletin of the Seismological Society of America, 65(5), pp. 1073–1095.

Kijko, A. (2004) Estimation of the maximum earthquake magnitude, Mmax. Pure and Applied Geophysics, 161(8), pp. 1655–1681.

Kijko, A. and Funk, C.W. (1994) The assessment of seismic hazards in mines. The Journal of The Southern African Institute of Mining and Metallurgy, 94(7), pp. 179–185.

Laplace, P.S. (1812) Théorie Analytique des Probabilités. Ve. Courcier, 464 pp.

Lomnitz, C. (1974) Global Tectonics and Earthquake Risk. Development in Geomechanics, Elsevier.

Main, I.G. and Burton, P.W. (1984) Information theory and the earthquake frequency-magnitude distribution. Bulletin of the Seismological Society of America, 74(4), pp. 1409–1426.

McGarr, A. (1976) Upper limit to earthquake size. Nature, 262(5567), pp. 378–379.

McGarr, A. (1984) Scaling of ground motion parameters, state of stress, and focal depth. Journal of Geophysical Research, 89(B8), pp. 6969–6979.

McGarr, A. (1993) Keynote Address: Factors influencing the strong ground motion from mining-induced tremors. In R.P. Young (ed.), Proceedings 3rd International Symposium on Rockbursts and Seismicity in Mines, Kingston, Ontario, Canada, Balkema, Rotterdam, pp. 3–12.

McGuire, R.K. (1977) Effects of uncertainty in seismicity on estimates of seismic hazard for the east coast of the United States. Bulletin of the Seismological Society of America, 67(3), pp. 827–848.

Mendecki, A.J. (1985) An attempt to estimate seismic hazard on the AAC gold mines. Special Report SP8/85, Anglo American Coorporation, Gold and Uranium Division, South Africa.

Mendecki, A.J. (2001) Data-driven understanding of seismic rock mass response to mining: Keynote Address. In G. van Aswegen, R.J. Durrheim and W.D. Ortlepp (eds.), Proceedings 5th International Symposium on Rockbursts and Seismicity in Mines, Johannesburg, South Africa, South African Institute of Mining and Metallurgy, pp. 1–9.

Mendecki, A.J. (2005) Persistence of seismic rock mass response to mining. In Y. Potvin and M.R. Hudyma (eds.), Proceedings 6th International Symposium on Rockburst and Seismicity in Mines, Perth, Australia, Australian Centre for Geomechanics, pp. 97–105.

Molnar, P. (1979) Earthquake recurrence intervals and plate tectonics. Bulletin of the Seismological Society of America, 69(1), pp. 115–133.

Oresme, N. (1482) Tractatus de configuratione qualitatum et motuum (Tractatus de configurationibus qualitatum et motuum: Questiones super geometriam Euclidis), published by Johannes de Sancto Martino.

Page, R. (1968) Aftershocks and microaftershocks of the great Alaska earthquake of 1964. Bulletin of the Seismological Society of America, 58(3), pp. 1131–1168.

Robson, D.S. and Whitlock, J.H. (1964) Estimation of a truncation point. Biometrica, 51(1-2), pp. 33–39.

Rodkin, M.V. and Pisarenko, V.F. (2006) Extreme earthquake disasters: Verification of the method of parameterization of the character of distribution of the rare major events. In W.H. Ip and Y.T. Chen (eds.), Advances in Geosciences Volume 1: Solid Earth (SE), World Scientific, pp. 75–89.

Saito, M., Kikushi, M. and Kudo, K. (1973) Analitical solution to Go-Game model inearthquakes. Zishin, 26(2), pp. 19–25.

Smith, S.W. (1976) Determination of maximum earthquake magnitude. Geophysical Research Letters, 3(6), pp. 351–354.

Somerville, P.G., Smith, N.F., Graves, R.W. and Abrahamson, N.A. (1997) Modifications of empirical strong ground motion attenuation relations to include the amplitude and duration effects of rupture directivity. Seismological Research Letters, 68(1), pp. 199–222.

Sornette, D. and Sornette, A. (1999) General theory of the modified Gutenberg-Richter law for large seismic moments. Bulletin of the Seismological Society of America, 89(4), pp. 1121–1130.

Tversky, A. and Kahneman, D. (1974) Judgment under Uncertainty: Heuristics and Biases. Science, 185(4157), pp. 1124–1131.

Tversky, A. and Kahneman, D. (1986) Rational choice and the framing of decisions. Journal of Business, 59, pp. S251–S278.

Vere-Jones, D. (1976) A branching model for crack propagation. Pure and Applied Geophysics, 114, pp. 711–726.

Vick, S.G. (2002) Degrees of Belief: Subjective Probability and Engineering Judgment. American Society of Civil Engineers Press, 1801 Alexander Bell Drive, Reston, Virginia 20191-4400.

Wyss, M. (1973) Towards a physical understanding of the earthquake frequency distribution. Geophysical Journal of the Royal Astronomical Society, 31(4), pp. 341–359.